Supplementary Information

Identification of a central role for complement in osteoarthritis

Qian Wang, Andrew L. Rozelle, Christin M. Lepus, Carla R. Scanzello, Jason J. Song, D. Meegan Larsen, James F. Crish, Gurkan Bebek, Susan Y. Ritter, Tamsin M. Lindstrom, Inyong Hwang, Heidi H. Wong, Leonardo Punzi, Angelo Encarnacion, Mehrdad Shamloo, Stuart B. Goodman, Tony Wyss-Coray, Steven R. Goldring, Nirmal K. Banda, Joshua M. Thurman, Reuben Gobezie, Mary K. Crow, V. Michael Holers, David M. Lee, and William H. Robinson

Supplementary Methods

Proteomic profiling of synovial fluids. We studied human samples under protocols that were approved by the Stanford Institutional Review Board (IRB) and included subjects' informed consent, and under protocols that were approved by Partners Healthcare IRB and did not require subjects' informed consent. We obtained synovial fluids from healthy individuals with no symptoms of knee osteoarthritis; patients with early-stage osteoarthritis with symptoms of <1 year's duration, as assessed by the presence of arthroscopically visible cartilage lesions or by radiographic imaging; and patients with end-stage osteoarthritis undergoing total knee joint replacement. We labeled synovial fluid proteins with Cy3 or Cy5, subjected them to isoelectric focusing (IEF), and separated them on acrylamide gels (2D-DIGE). We selected differentially expressed spots by using DeCyder software (GE Healthcare) based on expression change of ≥1.2 fold and a significant *t* test ($P < 0.05$). We determined protein identities by LC-MS/MS in conjunction with a Mascot database search (Matrix Science). We used OptEIA ELISA kits (BD Biosciences) to detect C3a and C5b-C9 in synovial fluids.

Spontaneous osteoarthritis in aged mice. We sacrificed male *Cd59a*$^{-/-}$ and wild-type C57Bl/B6 (Jackson Laboratories) mice at 18 months of age, and harvested their joints for histological scoring of safranin-O-stained sections, as described below.

Histological scoring of mouse arthritis. We stained fixed, paraffin-embedded, 4-μm-thick sections of decalcified mouse joints with toluidine blue, safranin-O, or hematoxylin and eosin (H&E). To evaluate osteophyte formation, we scored toluidine-blue-stained sections according to a previously described scoring system[1]: 0, none; 1, formation of cartilage-like tissues; 2, increase of cartilaginous matrix; 3, endochondral ossification. To assess spontaneous osteoarthritis in aged mice, we calculated a "histological score" by scoring sections stained with safranin-O, which allows detection of more subtle changes to the joint, such as proteoglycan loss in the absence of cartilage loss. We scored safranin-O-stained sections according to a modified version[2] of the Mankin scoring system[3]: 0, no damage; 1, irregular cartilage surface; 2, loss of safranin-O staining without structural changes; 3, loss of surface <20%; 4, severe loss of cartilage (>80%); 5, erosion down to the bone. To evaluate synovitis, we scored H&E-stained sections according to a previously described scoring system[4]: 0, no changes compared to normal joints; 1, thickening of the synovial lining and some influx of inflammatory cells; 2, thickening of the synovial lining and intermediate influx of inflammatory cells; and 3, profound thickening of the synovial lining (more than four cell layers) and maximal observed influx of inflammatory cells. Scores for osteophyte formation, synovitis, and "histological score" were recorded for the femoral-medial and the tibial-medial condyles on the operated side of the joint, and the scores for the two regions were summed.

Statistical Analysis. We analyzed “histological scores” by two-tailed unpaired *t* test, and osteophyte scores and synovitis scores by Mann-Whitney *U* test.

Supplementary Table 1. Complement proteins identified by 2D-DIGE and mass spectrometry as differentially expressed in synovial fluids from individuals with end-stage osteoarthritis (*n* = 10) compared to synovial fluids from healthy individuals (*n* = 10).

Proteins Identified	**Swiss-Prot Reference**
Complement component 1, s subcomponent	P09871
Complement component 3	P01024
Complement component 4A	P0C0L4
Complement component 4 binding protein, alpha	P04003
Complement component 5	P01031
Complement component 7	P10643
Complement component 9	P02748
Complement factor B	P00751
Complement factor H	P08603
Complement factor I	P05156
Clusterin	P10909
C1 inhibitor (encoded by serpin peptidase inhibitor; *SERPING1*)	P05155

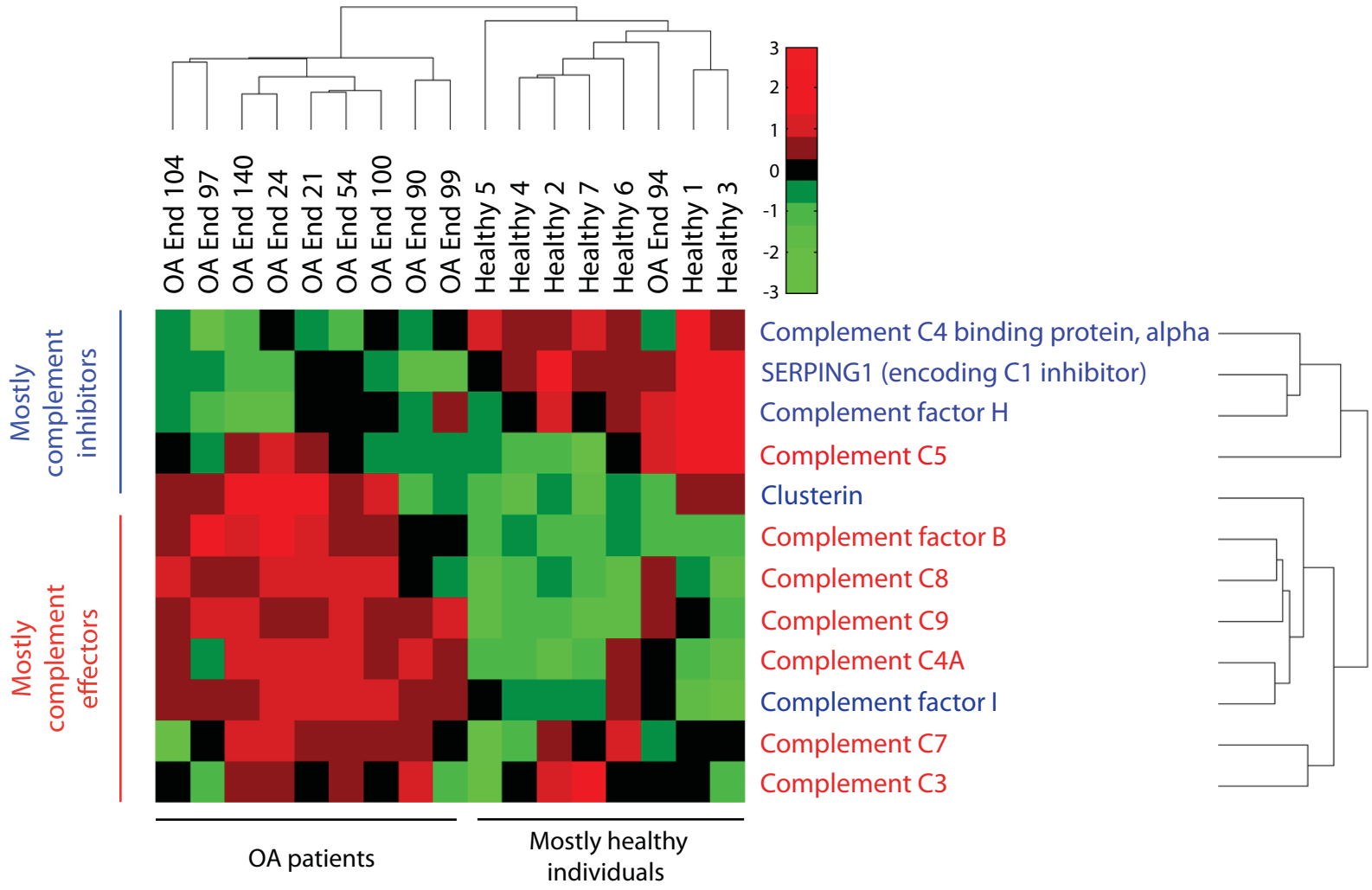

Supplementary Figure 1 Cluster analysis of gene-expression profiles in microarray datasets generated using synovial membranes from healthy individuals and from individuals with end-stage osteoarthritis (OA patients). Unsupervised hierarchical clustering was performed on the complement-related RNA transcript profiles of synovial membranes from healthy individuals and individuals with end-stage osteoarthritis (downloaded from the NCBI Gene Expression Omnibus, accession number GSE12021[5]), with analysis limited to the set of genes encoding the complement-related proteins shown in **Supplementary Table 1**. The scale bar represents fold change in gene expression compared to the reference control. Complement effectors are shown in red text, and complement inhibitors in blue text. Unsupervised hierarchical clustering of the GSE12021 data produced a result similar to that presented in **Fig. 1e**, with synovial membranes from healthy individuals expressing higher levels of genes encoding complement inhibitors, and synovial membranes from individuals with end-stage osteoarthritis expressing higher levels of complement effectors. The differences in the osteoarthritis datasets used in **Fig. 1e** and **Supplementary Fig. 1** result in differences in normalization and clustering, which in turn lead to subtle differences in the displayed fold changes in gene expression. Nevertheless, the overall pattern of a relative increase in expression of complement-effector genes, and a decrease in expression of complement-inhibitor genes, in individuals with osteoarthritis is seen in both datasets.

a

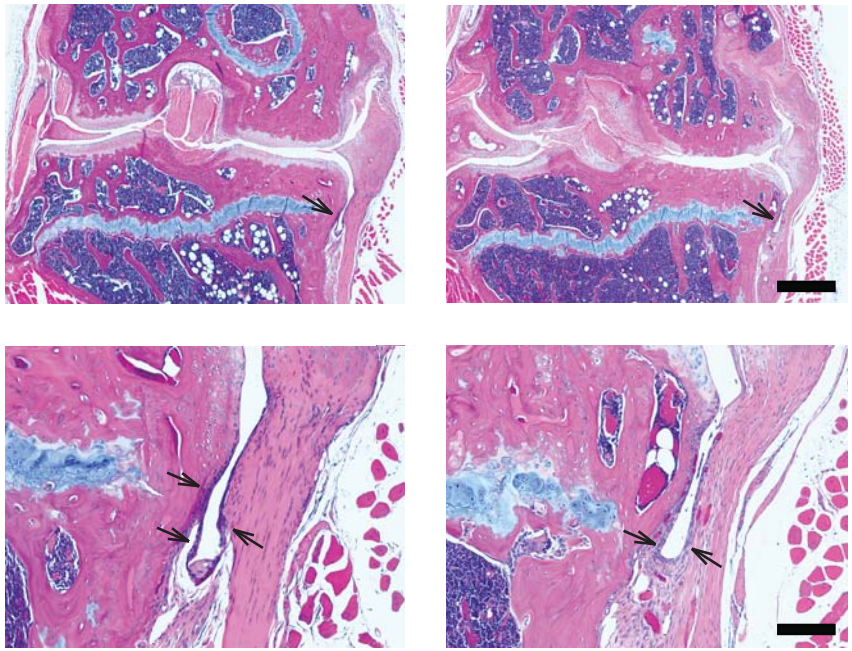

Cd59a$^{+/+}$ *Cd59a*$^{-/-}$

b

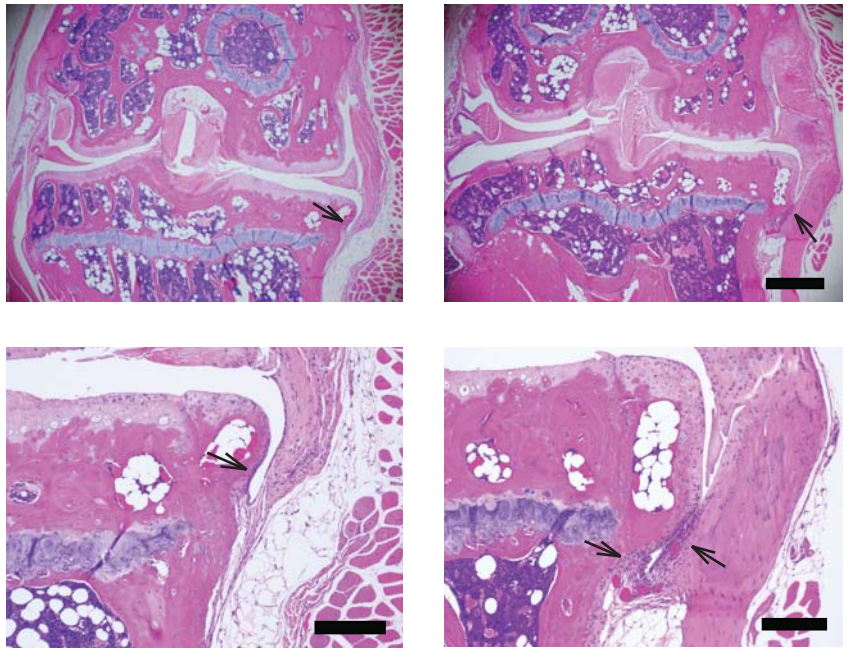

Cd59a$^{+/+}$ *Cd59a*$^{-/-}$

c

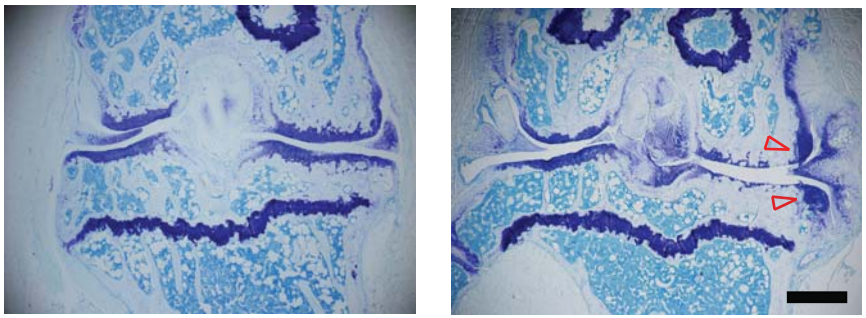

Cd59a$^{+/+}$ *Cd59a*$^{-/-}$

d

	C5 $^{+}$	C5 $^{-}$	C6 $^{+}$	C6 $^{-}$	*Cd59a* $^{+/+}$	*Cd59a* $^{-/-}$	*Cd59a* $^{+/+}$	*Cd59a* $^{-/-}$	*Cd59a* $^{+/+}$	*Cd59a* $^{-/-}$
Model	MM		MM		MM		DMM		Aging	
Osteophyte score*	4.00 ± 0.45	2.20 ± 0.20	4.17 ± 0.24	2.00 ± 0.20	3.73 ± 0.33	5.00 ± 0.24	2.00 ± 0.41	3.25 ± 0.25	0.60 ± 0.25	2.20 ± 0.58
***P* value**	0.016		< 0.0001		0.011		0.063		0.044	
Synovitis score*	2.20 ± 0.73	1.20 ± 0.73	2.77 ± 0.23	1.69 ± 0.31	2.30 ± 0.36	3.2 ± 0.25	1.00 ± 0.41	1.75 ± 0.48	0.00 ± 0.00	0.00 ± 0.00
***P* value**	0.257		0.013		0.053		0.353		N/A	

*Maximum score per joint: 6

Supplementary Figure 2

Supplementary Figure 2 Osteophyte formation and synovitis in mouse models of osteoarthritis. Representative H&E-stained sections of the medial region of stifle joints from *Cd59a*$^{-/-}$ and *Cd59a*$^{+/+}$ mice subjected to (**a**) medial meniscectomy (MM) or (**b**) destabilization of the medial meniscus (DMM). Arrows indicate areas of synovitis. Scale bars: low-magnification (top) images, 500 μM; high-magnification (bottom) images, 125 μm. (**c**) Representative toluidine-blue-stained sections of the medial region of stifle joints from *Cd59a*$^{-/-}$ and *Cd59a*$^{+/+}$ mice subjected to DMM. Arrowheads indicate osteophytes. (**d**) Osteophyte and synovitis scores for the mouse osteoarthritis experiments presented in **Fig. 2** and **Supplementary Fig. 3**. Quantification of osteophyte formation and synovitis in wild-type and genetically deficient mice in three different models of osteoarthritis. Osteophyte formation was scored on toluidine-blue-stained sections, and synovitis on H&E-stained sections. Data are the mean ± s.d. Statistical significance of differences was determined by Mann Whitney *U* test.

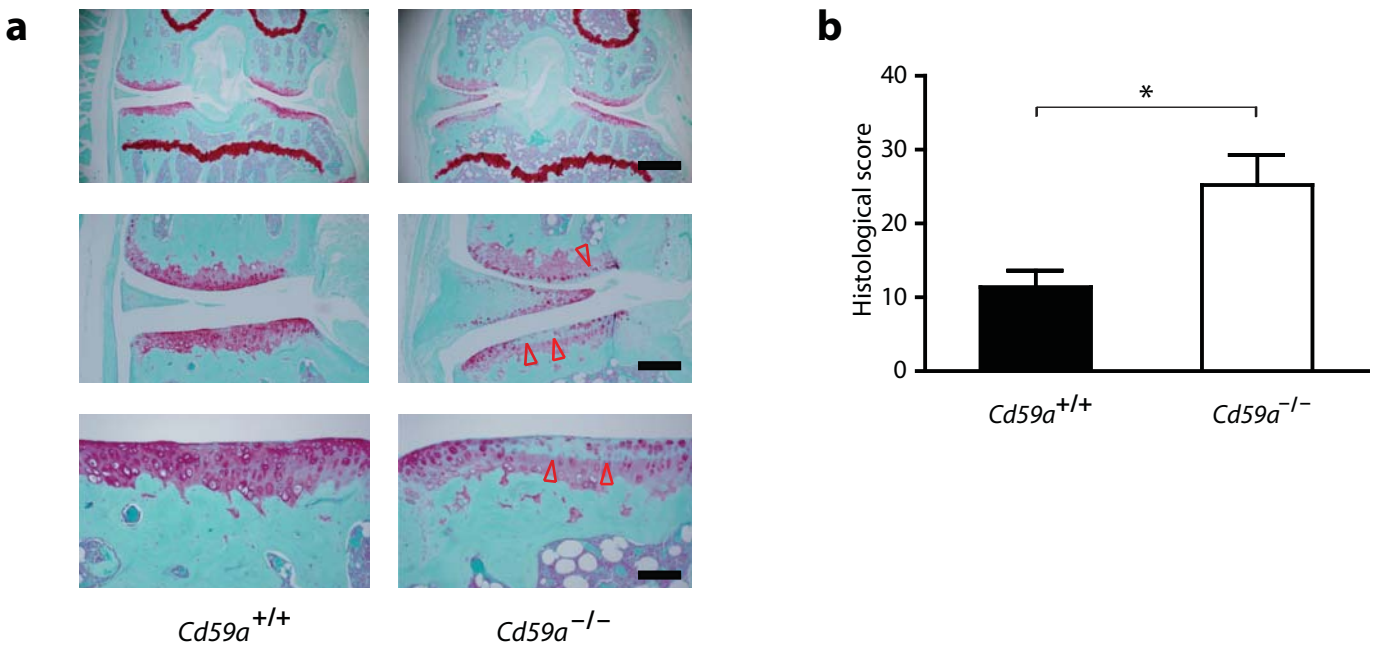

Supplementary Figure 3 Cd59a deficiency accentuates spontaneous osteoarthritis in aged mice. (**a**) Representative safranin-O-stained sections of the medial region of stifle joints of aged *Cd59a*$^{+/+}$ and *Cd59a*$^{-/-}$ mice developing spontaneous osteoarthritis. Arrowheads indicate areas of proteoglycan loss in (**a**). Scale bars: low-magnification (top) image, 500 μm; higher-magnification (middle) image, 200 μm; highest-magnification (bottom) image, 100 μm. (**b**) Quantification of histological osteoarthritis in (**a**) (n = 5 mice per group). Data are the mean + s.e.m. *P < 0.05, by t test.

a

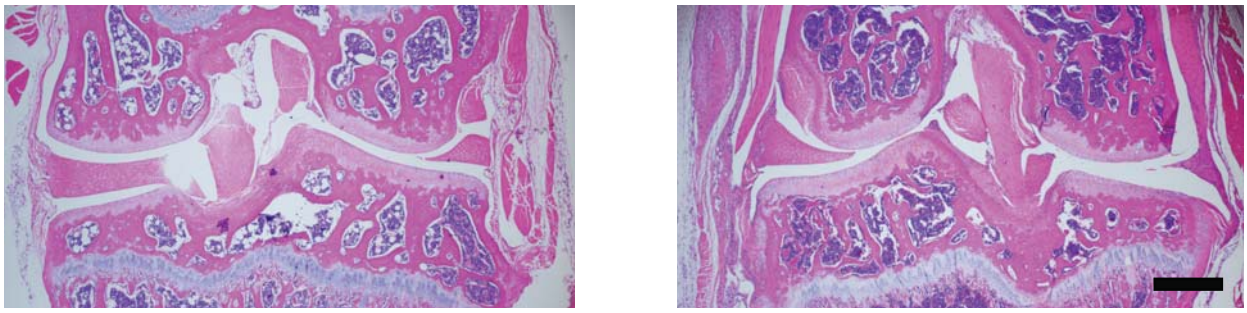

$C5^+$, week 2

$C5^-$, week 2

b

	2 weeks	4 weeks	8 weeks	12 weeks
$C5^+$ synovitis	0 ± 0	1.00 ± 0	1.25 ± 0.25	1.75 ± 0.25
$C5^-$ synovitis	0 ± 0	0 ± 0	0.50 ± 0.29	0.75 ± 0.25
P value	n/a	n/a	0.1336	0.0578

Supplementary Figure 4 Time course of synovitis in the medial meniscectomy model of osteoarthritis. (**a**) No signs of synovitis 2 weeks after surgery. Representative H&E-stained sections of the medial region of stifle joints from $C5^-$ and $C5^+$ mice 2 weeks after surgery. Scale bar, 500 μM. (**b**) Synovitis scores for the $C5^-$ and $C5^+$ mouse osteoarthritis experiments presented in **Fig. 3b**. Synovitis was scored on H&E-stained sections of the medial region of stifle joints. Data are the mean ± s.d. Statistical significance of differences was determined by Mann Whitney *U* test.

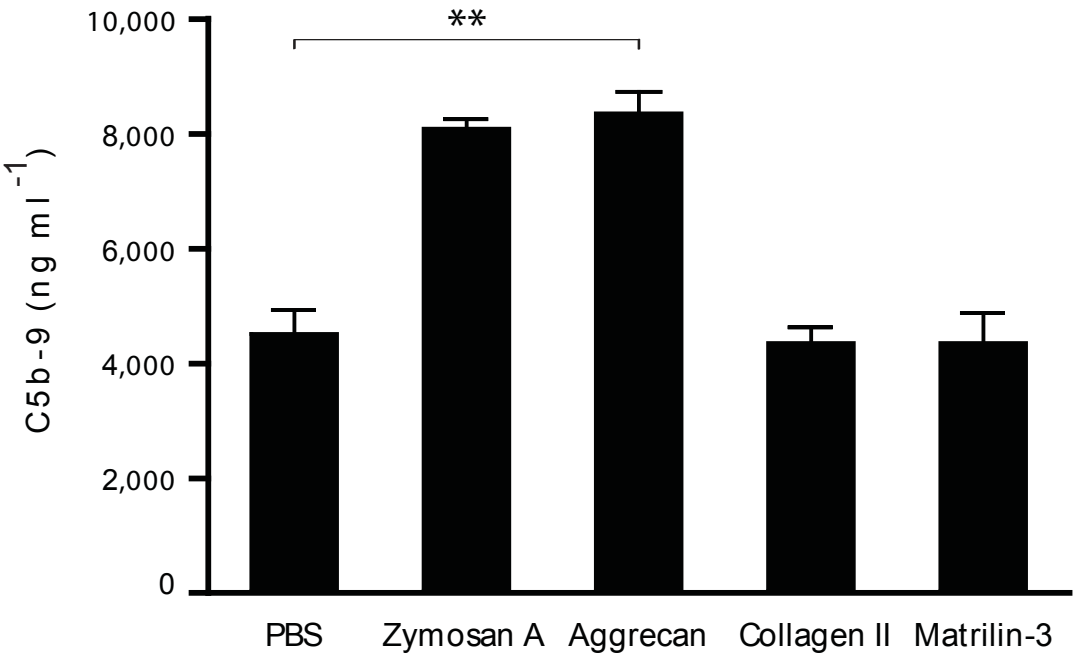

Supplementary Figure 5 The cartilage ECM component aggrecan can induce the formation of MAC. ELISA quantification of C5b-9 (soluble MAC) in 33% human serum incubated with 150 μM of bovine aggrecan, bovine collagen type II, or recombinant human matrilin-3. Zymosan A was used as a positive control, and the PBS diluent as a negative control. ** $P \leq 0.01$ by *t* test comparing aggrecan with PBS. Data are the mean of triplicate values ± s.d. and representative of three independent experiments.

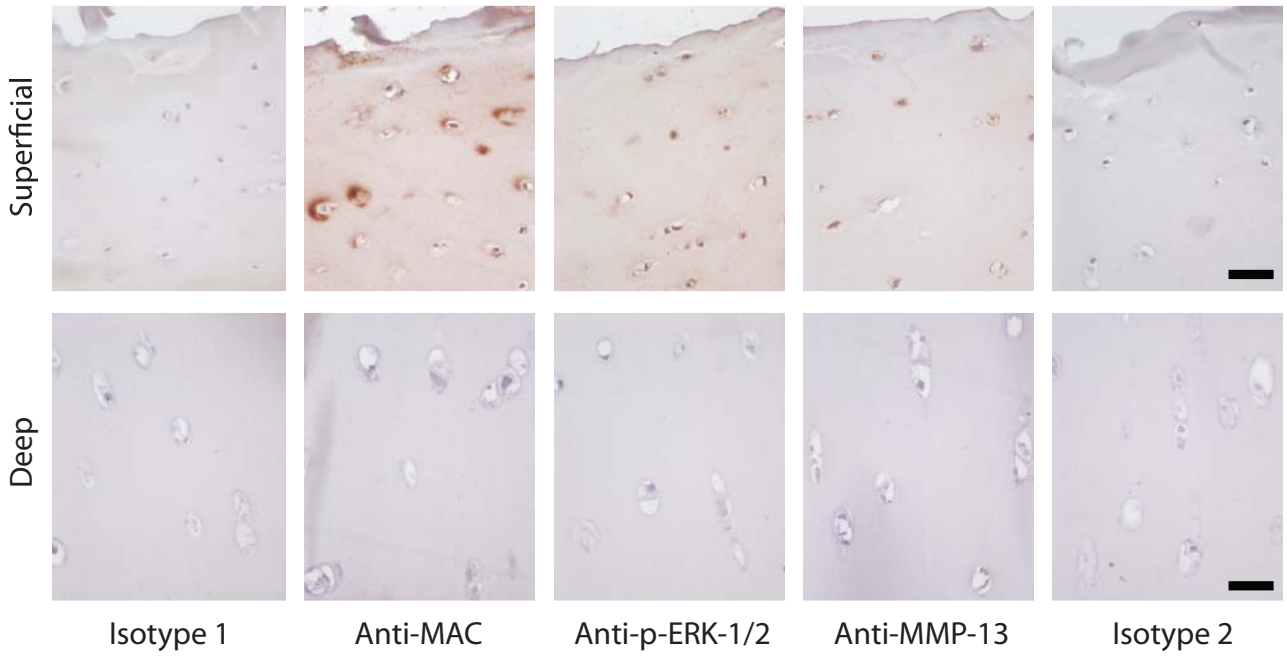

Supplementary Figure 6 MAC, phospho-ERK1/2, and MMP-13 show similar distribution patterns in cartilage from individuals with osteoarthritis. Immunohistochemical analysis of serial sections of human osteoarthritic cartilage shows that MAC, phospho-ERK1/2, and MMP-13 are confined to superficial, but not deep-zone, articular chondrocytes. Scale bar, 50 μm.

Supplementary References

1. **Kamekura, S.*, et al.* Osteoarthritis development in novel experimental mouse models induced by knee joint instability. *Osteoarthritis Cartilage* 13, 632-641 (2005).**
2. **Kadri, A.*, et al.* Osteoprotegerin inhibits cartilage degradation through an effect on trabecular bone in murine experimental osteoarthritis. *Arthritis Rheum* 58, 2379-2386 (2008).**
3. **Mankin, H.J., Dorfman, H., Lippiello, L. & Zarins, A. Biochemical and metabolic abnormalities in articular cartilage from osteo-arthritic human hips. II. Correlation of morphology with biochemical and metabolic data. *J Bone Joint Surg Am* 53, 523-537 (1971).**
4. **Blom, A.B.*, et al.* Synovial lining macrophages mediate osteophyte formation during experimental osteoarthritis. *Osteoarthritis Cartilage* 12, 627-635 (2004).**
5. **Huber, R.*, et al.* Identification of intra-group, inter-individual, and gene-specific variances in mRNA expression profiles in the rheumatoid arthritis synovial membrane. *Arthritis Res Ther* 10, R98 (2008).**